Phytomedicine 122 (2024) 155168

Contents lists available at ScienceDirect

Phytomedicine

journal homepage: www.elsevier.com/locate/phymed

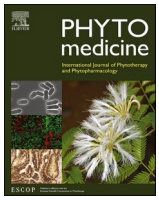

Original Article

Ginsenoside RK1 improves cognitive impairments and pathological changes in Alzheimer's disease via stimulation of the AMPK/Nrf2 signaling pathway

Lingyu She [a,c], Jinfeng Sun [c], Li Xiong [a], Ankang Li [d], Liwei Li [a], Haibin Wu [a,b], Juan Ren [a,b], Wei Wang [d], Guang Liang [a,b,*], Xia Zhao [a,b,*]

[a] Department of Pharmacy, Zhejiang Provincial People's Hospital, Affiliated People's Hospital, Hangzhou Medical College, Hangzhou, Zhejiang 310014, China
[b] Zhejiang TCM Key Laboratory of Pharmacology and Translational Research of Natural Products, School of Pharmaceutical Sciences, Hangzhou Medical College, Hangzhou, Zhejiang 310014, China
[c] Key Laboratory of Natural Medicines of the Changbai Mountain, Ministry of Education, Yanbian University, Yanji, Jilin 133002, China
[d] Affiliated Yongkang First People's Hospital, Hangzhou Medical College, Yongkang, Zhejiang 321399, China

ARTICLE INFO

Keywords:
Alzheimer's disease
RK1
Oxidative stress
AD-type pathologies
AMPK pathway

ABSTRACT

Background: The pathogenesis of Alzheimer's disease (AD) is complex, resulting in unsatisfactory effects of single-target therapeutic drugs. Accumulation evidence suggests that low toxicity multi-target drugs may play effective roles in AD. Ginseng is the root and rhizome of *Panax ginseng* Meyer, which can be used not only as herbal medicine but also as a functional food to support body functions. Ginsenoside RK1 (RK1), obtained from ginseng plants through high-temperature treatment, has antiapoptotic, antioxidant, anti-inflammatory effects and these events are involved in the development of AD. So, we believe that RK1 may be an effective drug for the treatment of AD.

Hypothesis/Purpose: We aimed to investigate the potential protective effects and mechanisms of RK1 in AD.

Methods: Neuronal damage was detected by MTT assay, LDH assay, immunofluorescence and western blotting. Oxidative stress was measured by JC-1 staining, reactive oxygen species (ROS) staining, superoxide dismutase (SOD) and malonaldehyde (MDA). The cognitive deficit was measured through morris water maze (MWM) and novel object recognition (NOR) tests.

Results: RK1 attenuated Aβ-induced apoptosis, restored mitochondrial membrane potential ($\Delta\Psi m$), and reduced intracellular levels of ROS in both PC12 cells and primary cultured neurons. *In vivo,* RK1 significantly improved cognitive deficits and mitigated AD-like pathological features. Notably, RK1 demonstrated superior efficacy compared to the positive control drug, donepezil. Mechanistically, our study elucidates that RK1 modulates the phosphorylation of AMP-activated protein kinase (AMPK) and its downstream target, NF-E2-related factor 2 (Nrf2), leading to the optimization of mitochondrial membrane potential, reduction of ROS levels, and mitigation of AD-like pathology. It's noteworthy that blocking the AMPK signaling pathway attenuated the protective effects of RK1.

Conclusion: RK1 demonstrates superior efficacy in alleviating cognitive deficits and mitigating pathological changes compared to donepezil. These findings suggest the potential utility of RK1-based therapies in the development of treatments for AD.

Abbreviations: Aβ, β-amyloid; AD, Alzheimer's disease; AMPK, AMP-activated protein kinase; AREs, antioxidant response elements; APP/PS1, APPswe/PSEN1dE9; DAPI, 4′,6-Diamidino-2′-phenylindole; DCFH-DA, Dichlorodihydrofluorescein diacetate; DMSO, Dimethyl sulfoxide; FITC, Fluorescein Isothiocyanate; FBS, Fetal bovine serum; HRP, horseradish peroxidase; IF, Immunofluorescence; JC-1, 5,5′,6,6′-Tetrachloro-1,1′,3,3′-tetraethyl-imidacarbocyanine; MDA, malonaldehyde; MTT, 3-(4,5-dimethylthiazol-2-yl)-2,5-diphenyl tetrazolium bromide; MWM, Morris water maze; NOR, New Object Recognition; PFA, Paraformaldehyde; PI, propidium iodide; PBS, phosphate buffered saline; PVDF, poly vinylidene fluoride; RT-qPCR, Real time quantitative Polymerase Chain Reaction; RIPA, Radio-Immunoprecipitation Assay; RK1, Ginsenoside RK1; ROS, reactive oxygen species; SDS-PAGE, sodium dodecyl sulfate polyacrylamide gel electrophoresis; SEM, standard error of mean; SOD, superoxide dismutase; TBST, Tris-buffered saline containing Tween; WT, Wild-type.

* Corresponding authors.
E-mail addresses: liangguang@wmu.edu.cn (G. Liang), xiazhao@hmc.edu.cn (X. Zhao).

https://doi.org/10.1016/j.phymed.2023.155168
Received 20 April 2023; Received in revised form 30 September 2023; Accepted 25 October 2023
Available online 30 October 2023

Introduction

Alzheimer's disease (AD) is a complex neurodegenerative disorder characterized by memory loss and cognitive decline (Fu et al., 2016; Yeung et al., 2015). The global aging population has increase the urgency of finding effective drugs in AD. β-amyloid (Aβ) is considered to be a core pathogenic component of AD (Gouras et al., 2005). During the development of AD, Aβ activates multiple secondary pathological processes, such as oxidative stress, tau hyperphosphorylation, neuroinflammation, and choline dysfunction (de Jesus de Paula et al., 2009). These second events promote each other and form a vicious circle that eventually causes neuronal death and AD symptoms (de Jesus de Paula et al., 2009).

Oxidative stress occurs in the early stages of AD and is directly linked to Aβ toxicity (Mota et al., 2015). Studies have shown that oxidative stress levels are high in the brains of AD patients (Markesbery, 1997). Furthermore, Aβ markedly elevates lipid peroxidation in the brain tissue of AD model mice, ultimately resulting in the generation of free radicals and consequent deficits in learning and memory (Moneim, 2015; Zhao et al., 2019). Therefore, the identification of prospective protective agents capable of modulating Aβ neurotoxicity and promoting antioxidation could represent a valuable strategy for AD treatment.

AMPK functions as a crucial energy sensor, serving as the primary regulator of cellular energy balance and oxidative stress (Daval et al., 2006; Hardie, 2008; Kemp et al., 2003). Activation of the AMPK cascade is associated with neuroprotective effects (Shukitt-Hale et al., 2015). AMPK has been suggested to modulate neurodegeneration by upregulating β-secretase 1 (BACE1) to increase the intracellular and extracellular Aβ production and directly phosphorylating tau (Hoover et al., 2010). Additionally, AMPK is activated in response to the presence of excess cellular ROS in AD (Kornelius et al., 2015). Nrf2 is a key transcription factor regulating antioxidant stress (Lu et al., 2022). AMPK phosphorylates Nrf2 and promotes its nuclear accumulation, activating antioxidant response elements (AREs) to restore cellular antioxidant capacity (Joo et al., 2016). Recently, Nrf2 activation by several drugs was found to attenuate oxidative stress and toxicity in Aβ1–42-induced AD cell models (Eftekharzadeh et al., 2010), suggesting that Nrf2 activation is a potentially effective treatment strategy for AD. Hence, targeting the AMPK/Nrf2 oxidative signaling pathways may lead to the development of new treatment and intervention strategies against Aβ neurotoxicity to further reduce brain damage in AD.

As the pathogenesis of AD is still unclear, many clinical drugs are ineffective or have serious side effects. Therefore, it is an urgent clinical need to find practical and effective therapeutic drugs. Currently, there is a growing interest in useful functional foods to prevent or delay AD (Zhang et al., 2019). Ginseng, sourced from the roots and rhizomes of *P. ginseng*, currently serves as a functional food renowned for enhancing bodily functions (Liu et al., 2016). Recent research has substantiated the capacity of ginsenosides to mitigate Aβ deposition and tau hyperphosphorylation, thereby ameliorating AD symptoms and retarding disease progression (Wu et al., 2022). RK1, derived from ginseng plants through high-temperature processing, possesses robust antioxidant and anti-inflammatory properties (Elshafay et al., 2017). Prior research has indicated its efficacy in ameliorating other neurodegenerative conditions, such as LPS induced depressive behavior (Li et al., 2020). But, its therapeutic effect and mechanism in AD remain poorly understood.

In this study, we employed an Aβ1–42-induced cell injury model and transgenic APP/PS1 mice to decipher the therapeutic effect and underlying mechanism of RK1 in AD. The outcomes demonstrated that RK1 mitigated oxidative damage and AD-related pathological through modulation of the AMPK/Nrf2 signaling pathway, offering novel prospects for AD therapy.

Materials and methods

Reagents

RK1 (DR0034) was bought from Chengdu DeSiTe Biological Technology. Donepezil (AB1619) was obtained from Chengdu Alfa Biotechnology Co., Ltd . Bovine Serum Albumin (BSA, 10,711,454,001), Dulbecco's modified Eagle's medium (DMEM, D0822) were procured from Sigma. Penicillin/Streptomycin was ordered from Gibco (Carlsbad, CA, USA). Dimethyl sulfoxide (DMSO, D2650) was procured from Sigma. Flow cytometry Apoptosis Detection Kit (556,570) was obtained from BD Biosciences (San Diego, CA, USA). PVDF membranes were bought from Bio-Rad (1,620,177). Fetal bovine serum (FBS) and 0.25 % Trypsin were obtained from Life Technologies (Grand Island, NY, USA). TUNEL staining kit (C1088), SOD (S0101S), GSH (S0057S), and MDA (S0131S) assay kit, MTT (ST316), JC-1 (C2006), Reactive Oxygen Species Assay Kit (S0033S), DAPI (P0131), and RIPA lysis buffer (P0013B) were bought from Beyotime Institute of Biotechnology (Shanghai, China). Aβ 1–42, with a molecular mass of 4514.10 (catalog number PA4391), having the sequence NH2-DAEFRHDSGYEVHHQKLVFFAEDVGSNKGAIIGLMVGGVVIA–COOH, was procured from Ontores Biotechnologies located in Zhejiang, China. Table S1 contains the comprehensive list of antibodies utilized in this study along with their respective sources. The table listing the primers utilized in this study is available in Table S2.

Animal treatment

APP/PS1 mice (APPswe, PSEN1dE9) were obtained from the Jackson Laboratory and accommodated in the animal facility at Hangzhou Medical College. They were kept under controlled conditions with a 12-hour light/dark cycle at 25 °C and had unrestricted access to food and water. The experimental protocol was approved by Hangzhou Medical College Animal Ethics Committee (2022–001). Female mice of equivalent age, body weight (approximately 30 g each), and age (8 months) were randomly assigned to one of five groups: WT, APP/PS1, APP/PS1 + 1 mg/kg RK1, APP/PS1 + 10 mg/kg RK1, and APP/PS1+ Donepezil. The drugs were prepared in a 2 % dimethyl sulfoxide (DMSO) solution in PBS. Before administration, mice in each group were individually weighed, and drug doses for intraperitoneal injection were adjusted according to their body weight. Intraperitoneal injections were administered daily for one month.

Preparation of tissue samples

After the behavioral assessments, mice from different experimental groups were euthanized with 100 mg/Kg Pentobarbital sodium. Subsequently, decapitation was performed following cardiac perfusion with 0.9 % saline. The brains of mice from each experimental group were carefully extracted, fixed in 4 % paraformaldehyde (PFA) at 4 °C for 24 h. Half of the brain samples were dehydrated by sucrose gradient, OCT embedding, and stored at -80 °C for subsequent IF analysis. Other brain tissue samples were placed in 1.5 ml tubes and preserved at -80 °C for future western blot analysis.

Morris water maze (MWM) test

One day before the experiment, the mice were moved to the behavior room and allowed to adjust to the environment. Briefly, mice were positioned within a water tank, and we recorded their escape time using an overhead video tracking system. If a mouse failed to locate the hidden platform within 60 s, the escape time was capped at 60 s (Bromley-Brits et al., 2011). On the fifth day, a spatial exploration task was performed by removing the hidden platform, allowing mice to swim freely for 60 s. The system recorded the number of times each mouse crossed the platform's previous location and the total time spent in each quadrant

(Vorhees and Williams, 2006). Data collection and analysis utilized the VisuTrack MWM image analysis system, located in Shanghai, China.

New object recognition (NOR) test

On the first day of the experiment, two identical objects A were put in the experimental setup. After the mice were put in, then the video equipment was turned on to record the contact situation of the mouse with the two objects, including the times of contact with the object and the time of exploration. The test duration is 5 min. After 24 h, replace one object A in the experimental device with object B, record the same index as the first day, and also record for 5 min with video equipment.

Cell culture and treatments

PC12 cells were cultured in 10 % DMEM medium (with 10 % FBS and 1 % penicillin/streptomycin) in a cell incubator at 37 °C and 5 % CO2. Change the medium every two to three days of culture and passage the cells with 0.25 % trypsin when they reach 90 % confluency.

Primary neurons were isolated from the brains of newborn C57BL/6 (C57) mice within 24 h following an established protocol (Giordano and Costa, 2011). Newborn mice were immersed in 75 % alcohol for 5 min to ensure disinfection before decapitation for euthanasia. The brain was meticulously dissected and rinsed with cold 1xHBSS. After careful removal of blood vessels and meninges under a microscope, the brain tissue was finely minced. Subsequently, enzymatic digestion was carried out with 0.1 % trypsin at 37 °C for 20 min. After terminating the digestion process, the cell suspension obtained was filtered using a device with a 0.45 μm pore size and subsequently centrifuged at 1000 g for 5 min to remove the supernatant. Following this, the cells were resuspended and placed on poly-d-lysine-coated plates in Neurobasal Medium with the addition of 1 % B27.

MTT assay

The effect of RK1 on cell viability was detected using the MTT assay (Kumar et al., 2018; Zheng et al., 2016). PC12 cells were subjected to the relevant drug treatments within 96-well plates. Following this, the cells were incubate with MTT solution (0.5 mg/ml, dissolved in blank medium). After 3–4 h incubation, the MTT medium was removed, and 100 μL of DMSO were added to each well to dissolve the blue formazan crystals. Absorbance at 570 nm was quantified using microplate readers.

ROS staining

Excess ROS damage cellular proteins, lipids, and DNA, leading to cellular damage, thus we used the fluorescent probe DCFH-DA (Beyotime, S0033S, China) to measure the effect of RK1 on intracellular ROS production. PC12 cells were treated with appropriate drugs, then the cells were incubated with 10 μM DCFH-DA reagent in blank DMEM medium for 60 min in the dark in 37 °C, and then fluorescence intensity was measured using an Infinite M200 PRO multimode microplate with excitation at 488 nm and emission at 525 nm.

TUNEL assay

TUNEL staining assay (C1090, Beyotime, Shanghai, China) was used to examine the effect of RK1 on Aβ1–42-induced cellular apoptosis. Following drug treatments, cells were seeded into 96-well plates, fixed using 4 % PFA for 15 min, and then exposed to a 0.3 % H2O2 solution (dissolved in 1x PBS) for 30 min. Subsequently, cells underwent incubation with a TUNEL reaction mixture (consisting of 45 liters of fluorescent labeling solution and 5 liters of TdT enzyme) for 1 h at 37 °C in darkness. TUNEL-positive cells (green fluorescence) were observed under a fluorescent microscope and counted. The apoptosis was calculated as a percentage of the total number of cells.

Test of mitochondrial membrane potential ($\triangle\psi m$)

To assess the influence of RK1 on mitochondrial membrane potential, we employed the JC-1 kit. PC12 cells were first plated in 96-well dishes and subjected to the relevant drug treatments. Afterward, the cells underwent incubation with a 1x JC-1 staining solution at a concentration of 10 μg/ml within a 37 °C cell incubator for 30 min. Subsequently, the following steps were carried out.

SOD, MDA, and GSH assay

We followed the manufacturer's instructions to conduct the assay. Brain tissue samples were briefly collected and processed using RIPA lysis buffer. SOD activity was determined using the WST-8 method, in which WST-8 reacts with superoxide anions catalyzed by xanthine oxidase, resulting in a water-soluble formazan dye that could be quantified at 450 nm. To measure MDA content, we carried out a colorimetric reaction involving MDA and thiobarbituric acid (TBA), producing a red product measurable at 532 nm. We also assessed glutathione reductase activity, which converts oxidized glutathione (GSSG) to reduced glutathione (GSH). GSH subsequently reacted with the chromogenic substrate DTNB, generating yellow TNB and GSSG, quantified at 412 nm to determine TNB production.

Immunofluorescence (IF)

Mouse brain tissue embedded in OCT was sliced into 20 μm sections. Following a 30-minute drying period at 42 °C, the sections were treated with 0.1 % Triton X-100 (diluted in 1 × PBS) for 10 min. Subsequently, they were rinsed with 1xPBS and blocked in a 10 % BSA blocking buffer (diluted in 1 × PBS) for 60 min at room temperature. A drop of primary antibody was applied to each section and left to incubate overnight at 4 °C. The following day, the sections were allowed to reach room temperature for 40 min, after which the primary antibodies were washed off using 1 × PBS. They were then exposed to the appropriate fluorescent secondary antibodies for 2 h at room temperature. After washing with 1xPBS, we mounted the slides using the SlowFade® anti-fade DAPI reagent and captured images using a Nikon A1 confocal microscope.

Flow cytometry

After drug treatment, PC12 cells were collected by centrifuge at 1000 rpm for 10 min. Following this, cells were washed two times with 1xPBS, and then resuspended in 185 μl of 1x binding buffer. For each treatment group, 5 μl of Annexin V-FITC and 10 μl of propidium iodide (PI) were added to the cell suspensions, which were subsequently incubated for 30 min in darkness at room temperature. Subsequently, PC12 cells with different treatment were collected and analyzed using flow cytometry software.

Western blot

Protein samples from brain homogenates or cells were lysed with RIPA buffer on ice for 30 min, and quantified using a BCA detection kit (23,225, Thermo Fisher). The samples were subsequently subjected to separation through SDS-PAGE polyacrylamide gel electrophoresis, and then the proteins on the gel were transferred to 0.22 μm PVDF membrane under the condition of 260 mA for 90 min. PVDF membranes were blocked with 5 % BSA for 50 min and incubated the membrane with primary antibody (1:1000) overnight at 4 °C. Following day, the PVDF membrane was washed 3 times with 1 × TBST to remove the primary antibody, and then incubated with HRP-conjugated secondary antibody for 2 h at room temperature. Immunoreactive bands were visualized using the Bio-Rad Gel Doc XR system after addition of ECL, and band intensities were quantified using Image J software.

Statistical analysis

The statistical analysis will be carried out with the software, GraphPad Prism 8 software (GraphPad Software in San Diego, CA). Error bars were included in the figures to represent the mean ± standard error of the mean (SEM). To determine statistical significance across multiple groups, we utilized either one-way or two-way analysis of variance (ANOVA), followed by Tukey's post-hoc test. $p < 0.05$ is considered as that the result has statistical significance.

Results

RK1 attenuates PC12 cell toxicity induced by Aβ1–42

To examine the protective effect of RK1 on PC12 cells, we initially evaluated its protective effect on Aβ1–42-induced cell death through MTT assay. Result showed that RK1 (Fig. 1A) demonstrated a dose-dependent protective effect against Aβ1–42-induced cell death (Fig. 1B). The protective effects of RK1 were further confirmed through LDH assay (Fig. 1C), DAPI staining (Fig. 1D,1E), and flow cytometry (Fig. 1F,1G). These results indicated that Aβ1–42 exposure significantly increased LDH release and apoptotic cells in PC12 cells, but pretreatment with 1.25 μM ginsenoside RK1 reversed these changes. Caspase-3 is a key player in the caspase cascade (Slee et al., 2001). Bcl2 acts as an anti-apoptotic protein, whereas Bax operates as a pro-apoptotic protein (Kale et al., 2018). Western blot results demonstrated that RK1 pretreatment markedly reduced the protein level of Bax and increased the protein level of Bcl2 (Fig. 1H,1I). Similar results were observed at the mRNA level for Bax and Bcl-2, as measured by RT-qPCR (Fig. 1J). Additionally, RK1 significantly increased the mRNA expression of PARP, an important apoptosis indicator (Fig. 1J). Collectively, these findings demonstrate that RK1 confers neuroprotection against apoptosis induced by Aβ1–42 in PC12 cells.

RK1 induces AMPK/Nrf2 signaling in correlation with the neuroprotective effect against Aβ1–42-induced oxidative damage

Oxidative stress is a significant mechanism through which Aβ exerts neurotoxic effects. Consequently, we assessed intracellular ROS levels and mitochondrial membrane potential ($\triangle\psi m$). ROS staining revealed a notable increase in intracellular ROS levels induced by Aβ1–42. However, RK1 treatment markedly mitigated this heightened intracellular ROS production initiated by Aβ1–42 (Fig. 1K and 1l). Mitochondria are the primary sites for ROS generation, and we evaluated $\triangle\psi m$ by measuring the ratio of red to green fluorescence after JC-1 staining in PC12 cells. In healthy cells, the dye forms red fluorescent aggregates within mitochondria, while in apoptotic cells, it transitions into green, fluorescent monomers located in the cytoplasm. The results demonstrated that RK1 reversed the alteration in mitochondrial membrane potential induced by Aβ1–42 (Fig. 1K and 1M). AMPK is a pivotal regulator of cellular energy metabolism, highly conserved, and crucial in governing oxidative stress and mitochondrial energy metabolism. Thus, we examined whether RK1 influenced the expression and signaling of this pathway concerning its neuroprotective effect. The results indicated that Aβ1–42 decreased the expression levels of p-AMPK and Nrf2, and this effect was counteracted by pre-treatment with RK1 (Fig. 1N–1P).

Blocking the AMPK pathway inhibits the protective effects of RK1

To further confirm the involvement of AMPK/Nrf2 signaling in the protective effects of RK1, we pretreatment PC12 cells with an AMPK inhibitor (Compound C) at a concentration of 2 μM for 60 min, aiming to inhibit the AMPK pathway. Obtained result showed that the phosphorylation of AMPK (P-AMPK) was noticeably blocked following 2 μM Compound C pretreatment (Fig. 2A and 2B). Subsequently, we assessed oxidative stress using JC-1 and ROS staining (Fig. 2C–2E), evaluated cell viability through the MTT assay (Fig. 2F), quantified cell apoptosis by flow cytometry (Fig. 2G and 2H) and gauged the expression levels of apoptosis-related factors using western blotting (Fig. 2I and 2J). These findings consistently indicated that blocking AMPK significantly inhibited the protective effect of RK1 against Aβ1–42-induced oxidative stress and apoptosis, indicating that the AMPK signaling pathway was involved in the protective effect of RK1 against Aβ1–42-induced neurotoxicity..

RK1 improves the cognitive deficit in APP/PS1 CE mice

RK1 was administered via intraperitoneal injection once daily for 4 weeks. The treatment included a low dose of 1 mg/kg and a high dose of 10 mg/kg. Donepezil, a drug approved for AD clinic treatment, was administered at a dose of 5 mg/kg (Adlimoghaddam et al., 2018), and was used as a positive control drug in present experiments. Following this treatment period, the evaluation of learning and memory capacities was conducted through a NOR test (Fig. 3A,3B). The movement trajectory (Fig. 3C), number of novel object explorations (Fig. 3D), average speed (Fig. 3E), number of approaches (Fig. 3F), and total duration of approaches (Fig. 3G) of mice in each group were recorded. The results indicated that after treatment with RK1 or donepezil, there was an increase in the exploration of novel objects compared to the APP/PS1 group. We further verified these results using the MWM test. We recorded the movement trajectories of each mouse group (Fig. 3H and 3I). Notably, the average escape latency was substantially increased in APP/PS1 mice, indicative of decreased memory. However, after treatment with RK1 or donepezil, the average escape latency markedly decreased compared to the APP/PS1 group (Fig. 3J). Moreover, upon removal of the platform, both the RK1 and donepezil-treated groups exhibited a greater amount of time spent crossing the platform and remaining in the target quadrant in comparison to the APP/PS1 group (Fig. 3K and 3l). Significantly, RK1 demonstrated superior effectiveness in ameliorating cognitive impairments in APP/PS1 mice when compared to donepezil.

RK1 treatment promotes AD-type pathology

Aβ accumulation, neuroinflammation, and Tau phosphorylation are prominent hallmarks of AD. To investigate the impact of RK1 on Aβ accumulation, we performed Immunofluorescence. As anticipated, mice receiving RK1 or donepezil displayed reduced Aβ deposition (Fig. 4A). Neuroinflammation is primarily characterized by glial cell activation. To investigate RK1′s effect on neuroinflammation, we conducted IF for microglial markers (Iba1) and astrocyte markers (GFAP) in brain tissue, comparing it with the APP/PS1 group. Notably, RK1 and donepezil administration markedly suppressed microglial and astrocyte activation (Fig. 4A). To corroborate these findings, we conducted western blot analysis on brain homogenates using the same antibodies to assess levels of APP/β-amyloid and phosphorylated tau (P-tau). The results demonstrated a substantial reduction in APP/β-amyloid expression and tau phosphorylation following RK1 or donepezil treatment when compared to the untreated APP/PS1 group (Figs. 4B-4D). Importantly, it's noteworthy that RK1, administered at a dose of 10 mg/kg, exhibited superior efficacy in ameliorating AD pathology compared to the positive control drug, donepezil. Fig. 5

RK1 attenuates neuronal cell injury and oxidative stress in correlation with the activation of the AMPK/Nrf2 pathway

Reducing neuronal apoptosis is a critical objective in the neuroprotective treatment of AD. To assess the impact of ginsenoside RK1 on neuronal apoptosis in the brain, NeuN-labeled neuronal cells were initially employed for IF staining. RK1 and donepezil treatment ameliorated neuronal apoptosis in the hippocampus and cortex of APP/PS1 mice (Fig. 6A). We observed that RK1 treatment significantly

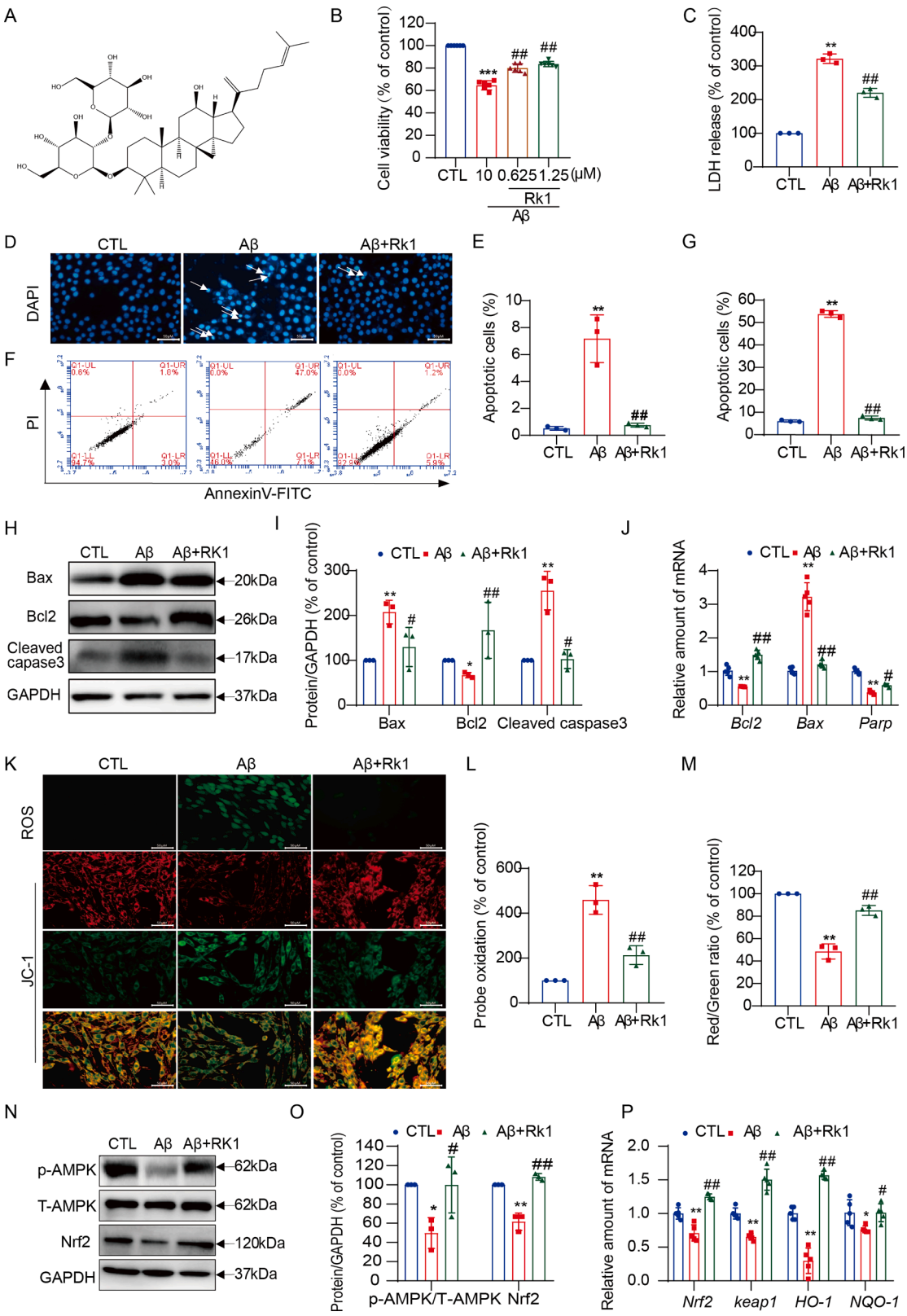

Fig. 1. Ginsenoside Rk1 reduced Aβ1–42-induced neurotoxicity in PC12 cells and activated AMPK/Nrf2 signaling.
(A) Chemical structure of Ginsenoside Rk1. (B) Cell viability in PC12 cells was measured using the MTT assay. (C) Cell damage was measured by LDH release assay. (D)Apoptotic cells were measured by DAPI staining. (E) Quantitation of apoptotic cells in D. (F) Apoptosis was tested by flow cytometry. (G) Quantitative analysis of (F). (H)Western blot analysis of cleaved caspase-3, Bax, and Bcl-2 in PC12 cells. (I) Quantitative data of the western blot intensity by Image J software. (J) mRNA levels of Bax, Bcl-2, and Parp in the PC12 cells were measured by Q-PCR. (K) The fluorescent images represent the ROS level as determined by the probes DCFH-DA and JC-1 dyes. (l) Quantitation of the percentage of the cellular ROS level. (M) Red to green fluorescence intensity ratio in different groups. (N) Expression of p-AMPK; T-AMPK and Nrf2 were detected by using Western blot. (O) Quantification of p-AMPK; T-AMPK and Nrf2. (P) RT -qPCR showing mRNA levels of Nrf2, keap1, Ho1, and Nqo1 in the PC12 cells. Results are presented as mean ± SEM ($n = 3$).

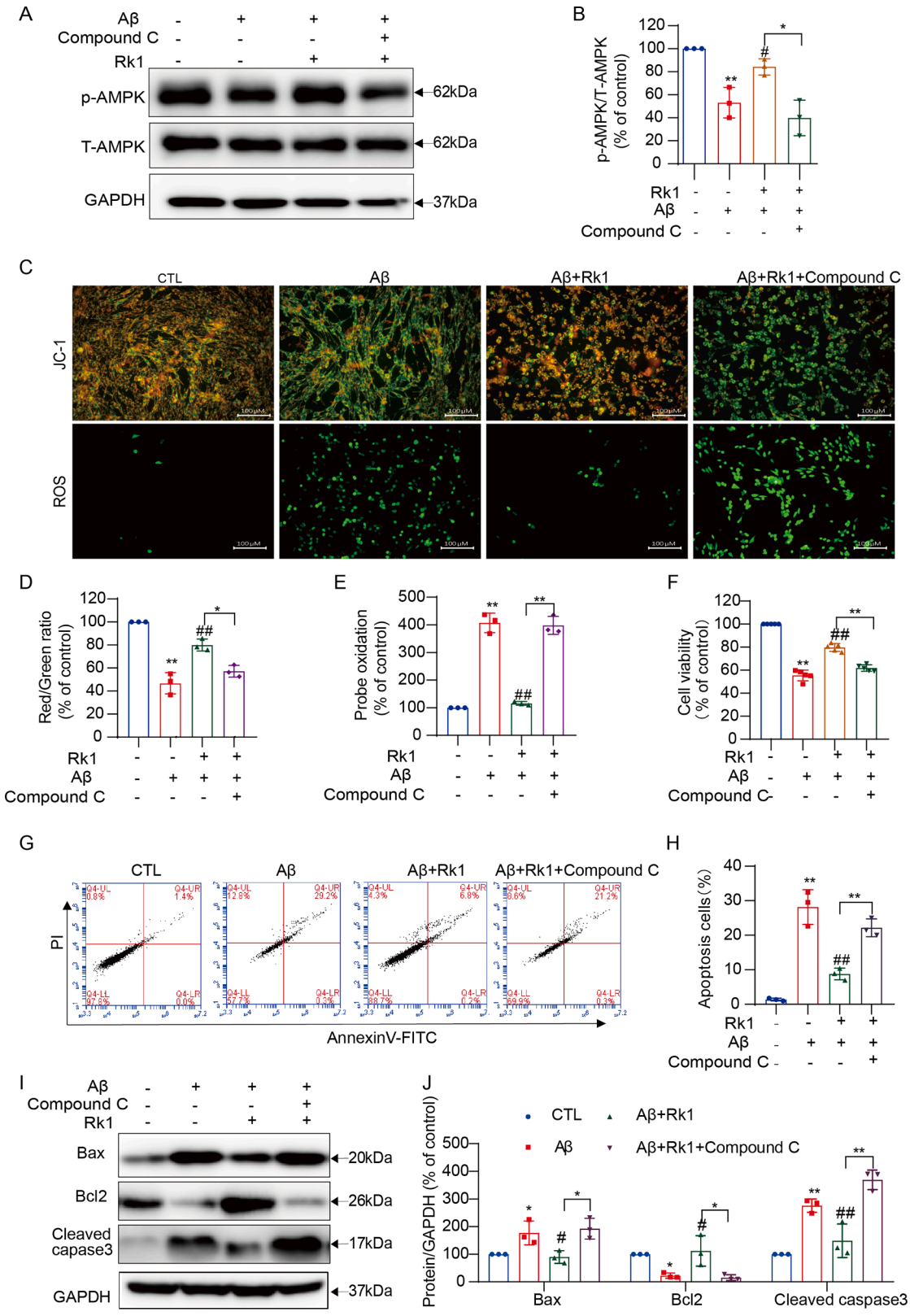

Fig. 2. The protective Effects of Ginsenoside Rk1 in PC12 Cells were reversed by AMPK inhibitor.
(A) Western blot analysis of p-AMPK and T-AMPK in PC12 cells. (B) Quantitative data of the blot intensity of corresponding proteins were determined by Image J software in-plane A. (C) The fluorescent images represent the ROS level as determined by the probes DCFH-DA and by staining the cells with JC-1 dyes. (D) Quantitation of the percentage of the cellular ROS level. (E) Red to green fluorescence intensity ratio (increase of mitochondrial membrane potential). (F) Cell viability was measured using the MTT. (G) Representative flow cytometry images. (H) Quantitation of the percentage of cell apoptosis. (I) Western blot analysis of Bax, Cleaved caspase-3, and Bcl2 in PC12 cells. (J) Quantitative data of the blot intensity of corresponding proteins were determined by Image J software in-plane A. Results are presented as mean ± SEM ($n = 3$).

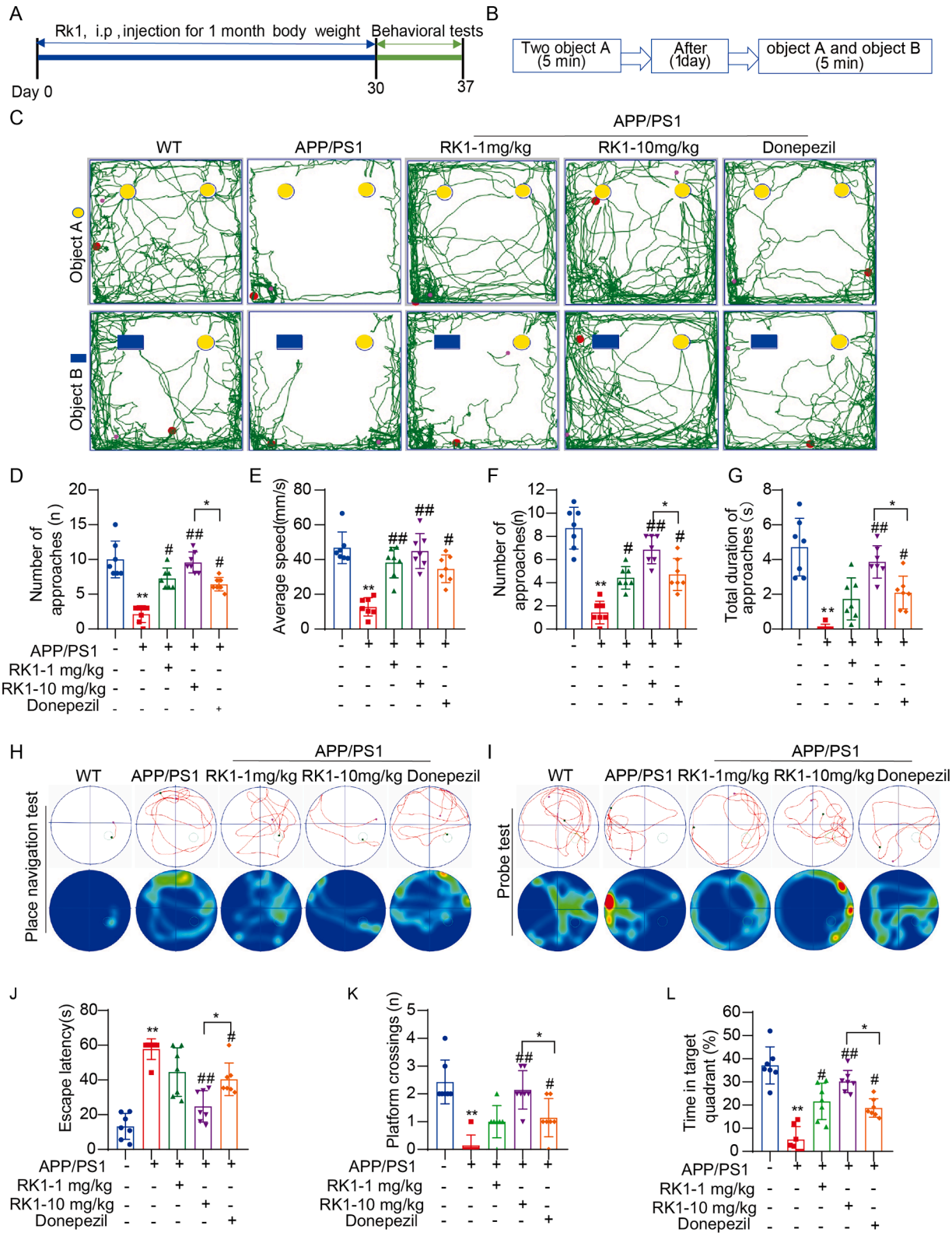

Fig. 3. Ginsenoside Rk1 improved the cognitive deficits of APP/PS1 mice.
(A) 8-month-old APP/PS1 mice were administered Ginsenoside Rk1 by intraperitoneal injection once a day. (B) flowchart of novel object recognition experiment. (C) The representative curve of novel object recognition experiments. (D) Preference for things on the first day of the new object recognition test. (E) Average speed on the first day of the new object recognition test. (F) A number of new object approaches of the new object recognition test. (G) The number of new object approaches of the new object recognition test. (H) Representative curve of place navigation test. (I) Representative curve of probe test. (J) Time is required to find the hidden platform. (K) The average crossing platform times of each group of mice within 60 s. (E) Time spent in the target quadrant where the platform had been located. Data are presented as mean ± SEM of $n = 7$ mice per group.

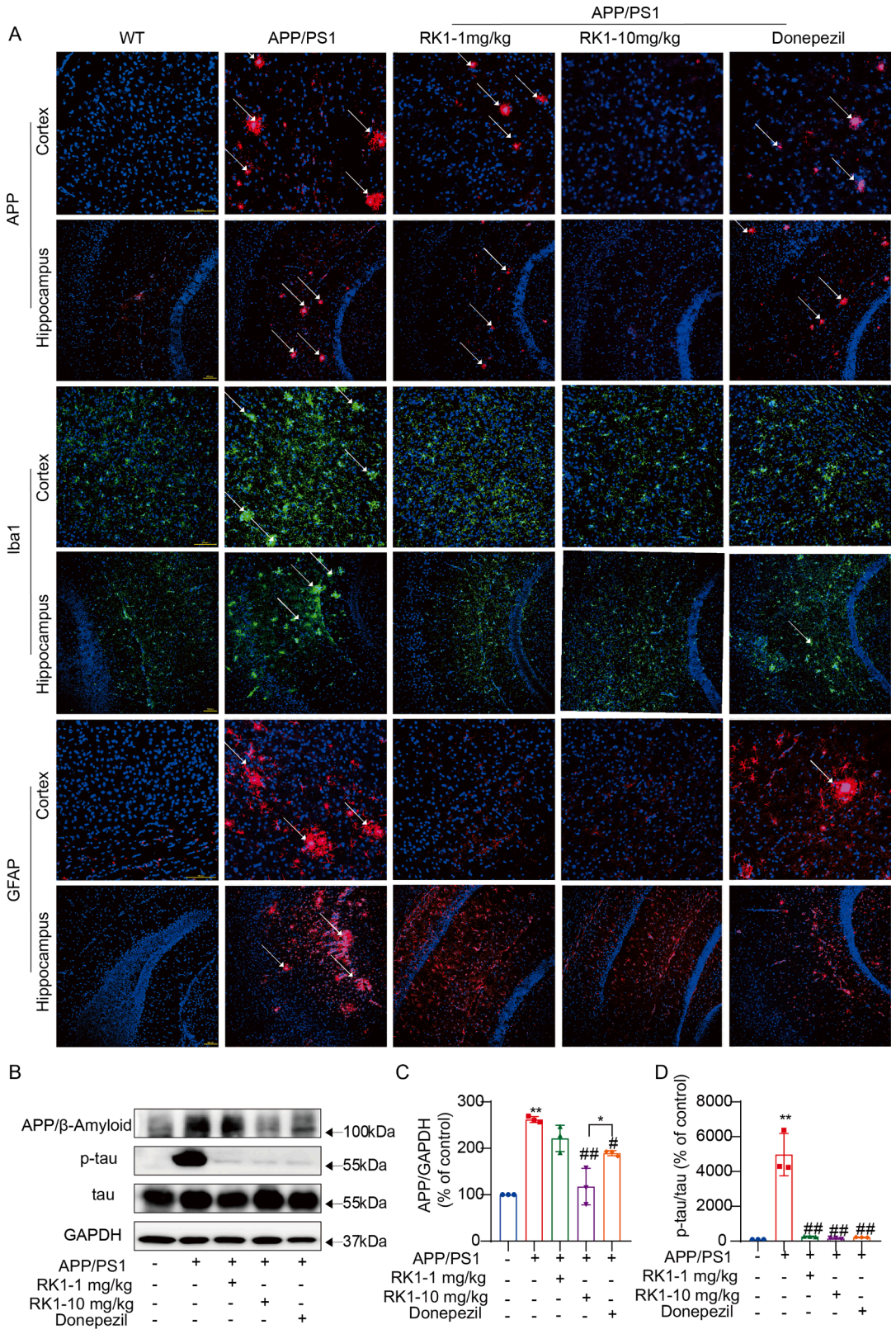

Fig. 4. Ginsenoside Rk1 treatment promoted AD-type pathology.
(A) Representative images of immunofluorescence in the hippocampus CA1 of 3 groups of mice at 8 months old. Scale bar = 100 μm. (B) Representative Western blot analysis of APP, p-Tau, and Tau in the hippocampus. (C-D) Quantitative data of the blot intensity of corresponding proteins were determined by Image J software in-plane A. Results are presented as mean ± SEM ($n = 3$).

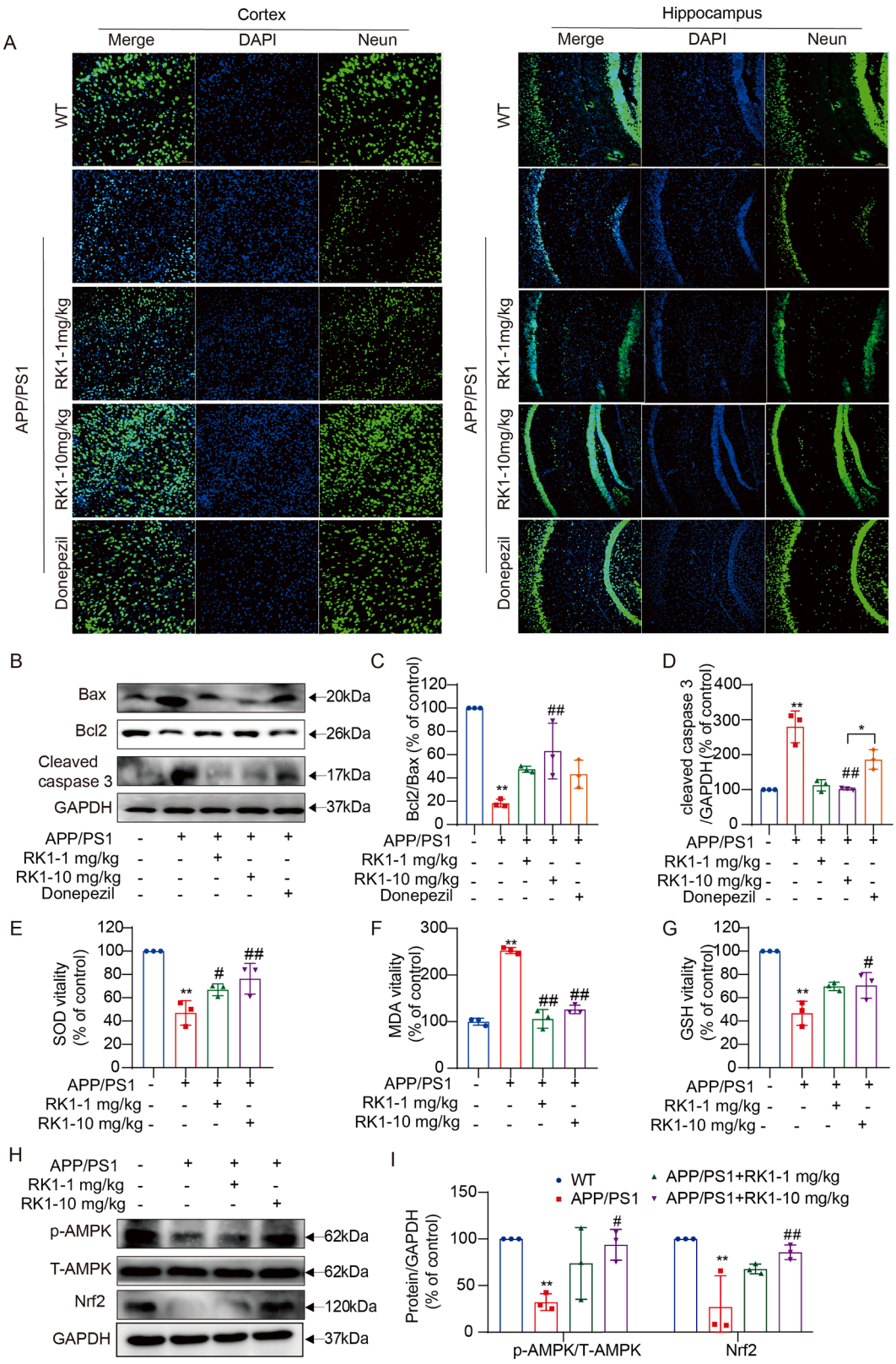

Fig. 5. Ginsenoside Rk1 attenuated neuron damage in APP/PS1 mice via activation of AMPK.
(A) Representative images of immunofluorescence in the hippocampus and cortex of 3 groups of mice at 8 months old. (B) Representative Western blot analysis of Bax, Bcl2, and Cleaved caspase3 in the hippocampus. (C) Quantitative data of the blot intensity of corresponding proteins were determined by Image J software in-plane A. (D) Quantitative data of the blot intensity of corresponding proteins were determined by Image J software in-plane A. (E-G) SOD, MDA, and GSH levels in the hippocampus were determined using biochemical kits respectively. (H) Representative Western blot analysis of p-AMPK and T-AMPK in the hippocampus. (I) Quantitative data of the blot intensity of corresponding proteins were determined by Image J software in-plane A. Results are presented as mean ± SEM ($n = 3$).

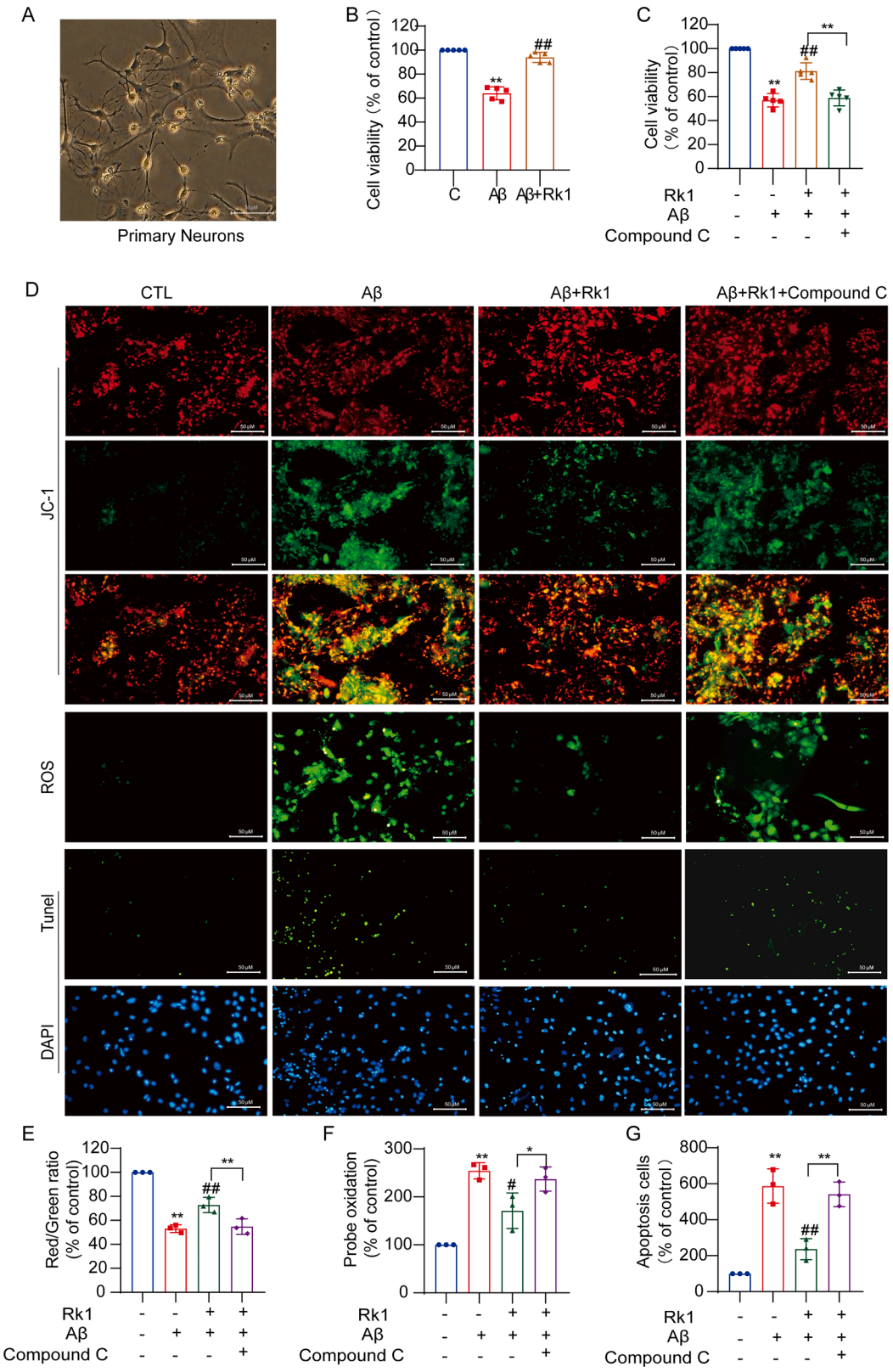

Fig. 6. Ginsenoside Rk1 conferred neuroprotection against Aβ1–42 induced injury in primary cultured neurons via the AMPK pathway.
(A) Representative images of primary neurons. (B-C) Cell viability was measured using the MTT assay. (D) The fluorescent images represent the ROS level as determined by the probes DCFH-DA, which determined mitochondrial membrane potential by staining the cells with JC-1 dyes and TUNEL staining. (E)Red to green fluorescence intensity ratio. (F) Quantitation of the percentage of the cellular ROS level. (G) Quantitation of TUNEL staining data. Results are presented as mean ± SEM ($n = 3$).

elevated the Bcl2/Bax ratio and reduced cleaved caspase 3 expression compared to untreated APP/PS1-AD mice, with a more pronounced effect than donepezil (Fig. 6B–D).

We investigated the impact of RK1 on oxidative stress *in vivo*. To assess oxidative stress, we quantified biomolecular damage byproducts, which included MDA, a well-established marker of lipid peroxidation. Additionally, we assessed the activity of SOD and measured the levels of GSH, a critical antioxidant enzyme vital for safeguarding the brain against damage caused by free radicals. As illustrated in Fig. 6E–6G, APP/PS1-AD mice exhibited significant deviations in MDA levels, SOD activity, and GSH levels when compared to their wild-type counterparts, indicating an elevated state of oxidative stress. Remarkably, treatment with a high dose of ginsenoside RK1 led to a substantial reversal of MDA and SOD levels in the brain extracts of APP/PS1-AD mice. These findings provide further substantiation of the antioxidative properties of ginsenoside RK1, which effectively impedes brain apoptosis and alleviates cognitive deficits in the APP/PS1 mouse model. Additionally, we assessed the phosphorylation of AMPK and Nrf2 in brain extracts from various experimental groups. P-AMPK and Nrf2 were reduced in the brains of APP/PS1-AD mice compared with WT mice, whereas RK1 treatment increased the expression of these proteins (Fig. 6H,6I). These findings confirm the results *in vitro*.

RK1 confers neuroprotection against Aβ1–42-induced apoptosis and oxidative stress in primary cultured neurons via the AMPK pathway

To further validate RK1′s protective effects, we isolated primary neuronal cells from the brains of newborn C57 mice (within 24 h) (Fig. 6A). These neurons were pre-treated with 1.25 μM RK1 for 24 h and subsequently exposed to 10 μM Aβ1–42 for an additional 24 h. Our findings demonstrate that RK1 significantly improved the reduced cell viability induced by Aβ1–42 in primary cultured neurons (Fig. 6B). To further substantiate RK1′s protective effect against Aβ1–42-induced oxidative stress and apoptosis in primary cultured neurons, we conducted a comprehensive evaluation encompassing cell viability, mitochondrial membrane potential *(Δψm)*, intracellular ROS levels, and apoptosis. These evaluations were carried out utilizing the MTT assay (Fig. 6C), JC-1 staining, quantification of ROS, and TUNEL staining (Fig. 6D). Significantly, the protective influence of RK1 was mitigated upon the introduction of AMPK inhibitors in primary neuronal cells. Importantly, these findings align consistently with outcomes observed in PC12 cells and the APP/PS1 mouse model, collectively reinforcing the notion that RK1 shields neuronal cells from oxidative stress through AMPK pathway activation.

Discussion

In the present research, we demonstrated for the first time that RK1 exerts effective therapeutic effects against AD, which is better than that of the available drug, donepezil. Our research shows that RK1 can reduce intracellular ROS levels and restore △ψm and apoptosis caused by Aβ1–42 in PC12 cells and primary cultured neurons. Further studies have shown that RK1 stimulates the AMPK/Nrf2 pathway. Incubation with Compound C weakened the protective effects of RK1. Similarly, the APP/PS1 mice model results showed that RK1 improved cognitive deficits and AD-type pathology in correlation with the activation of AMPK/Nrf2. Taken together, these results suggest a new potential drug candidate for the treatment of AD.

Given the multifaceted and intricate nature of AD pathology, the pursuit of traditional Chinese medicine compounds, renowned for their diverse pharmacological activities, is poised to yield innovative AD therapeutics (Pei et al., 2020). Ginseng, obtained from the root and rhizome of *P.* ginseng, is widely employed both in medicinal applications and as a functional dietary supplement to improve physiological functions (Patel and Rauf, 2017). Recent research indicates that ginseng extract, specifically its active component ginsenosides (also known as ginseng saponins), can ameliorate symptoms and impede the advancement of AD in afflicted individuals by diminishing the deposition of Aβ and tau (Kim et al., 2018). Ginsenoside Rg3 mitigated cognitive impairment in rats with AD by enhancing mitochondrial function (Zhang et al., 2019). RK1, derived through high-temperature processing of ginseng (Lee, 2014), exhibits a range of pharmacological benefits encompassing antioxidative, anti-inflammatory, anti-insulin resistance, neuroprotective, antibacterial, and anti-lipid accumulation effects (Elshafay et al., 2017). All the results above support the clinical protective effects of RK1 and demonstrate the potential of developing RK1-based treatments for the previously mentioned conditions. In this study, we discovered a new role for RK1 as a potential drug for the treatment of AD. At present, patients primarily rely on tacrine, donepezil, rivastigmine, and galantamine for cognitive deficit improvement, representing the mainstay of treatment. Remarkably, our findings indicate that RK1 exhibits a superior therapeutic effect compared to donepezil.

RK1 exhibits antioxidant effects (Pu et al., 2021). In this study, we found that Aβ1–42 caused a decrease in △*ψm* and an increase in intracellular ROS levels *in vitro*, while treatment with RK1 significantly inhibited these changes. Similarly, RK1 administration significantly increased SOD activity and concurrently decreased MDA activity in the brains of APP/PS1-AD mice. These findings strongly suggest that the antioxidant properties of RK1 may be the basis for its neuroprotective effects, both *in vivo* and *in vitro*. Neuronal cells in the brain contain a large amount of easily oxidized polyunsaturated fatty acids and have high rates of oxygen consumption, making them particularly vulnerable to oxidative damage (Halliwell, 2006). Activation of endogenous antioxidant defense systems, such as Nrf2, is required to combat oxidative stress-induced damage to brain neurons. Under oxidative stress, p-Nrf2 trans locates into the nucleus, forms a dimer with Maf, and promotes the expression of enzymes encoding antioxidant activities like HO-1 and SOD (Johnson and Johnson, 2015). In this study, we verified that RK1 activated Nrf2 and its downstream HO-1 while exerting its antioxidant and neuroprotective effects in PC12 cells and APP/PS1-AD mice. Activation of Nrf2 has been reported to prevent Aβ-mediated neurotoxicity in neuronal cell cultures (Sandberg et al., 2014). Gracilins A and C (sponge-derived diterpenoids) have been reported to significantly improve learning and memory in 3 × Tg mice by activating Nrf2 (Leirós et al., 2015).

Reduced AMPK activity has been observed in the brains of AD patients, indicating a corresponding decline in mitochondrial biogenesis and function (Dong et al., 2016). Activation of AMPK holds promise for ameliorating the brain's energy metabolism disruptions associated with AD pathogenesis and represents a potential therapeutic target (Cai et al., 2012). It's worth noting that oxidative stress impacts AMPK phosphorylation. Subsequently, AMPK phosphorylates Nrf2, facilitating its nuclear accumulation and the transactivation of ARE-driven genes (Joo et al., 2016). This process empowers cells to restore their antioxidant capacity. Our *in vitro* experiments and investigations in AD transgenic mice suggest that RK1 provides neuronal antioxidant protection by activating the AMPK/Nrf2 pathway, offering potential benefits for AD treatment. This study underscores the therapeutic potential of RK1 in AD. Nonetheless, further research is warranted to elucidate the mechanism by which RK1 modulates AMPK, as well as its bioavailability and pharmacokinetics.

In conclusion, this study shows that RK1 is more effective than donepezil in improving the symptoms of AD. Mechanistically, we found that the effect of RK1 was accompanied by activation of the AMPK signaling pathway in PC12 cells and APP/PS1 mouse models. Taken together, the present results reveal the great potential of RK1 as a new therapeutic drug candidate for AD treatment.

Author contributions

Xia Zhao, Guang Liang, and Wei Wang contributed to the literature

search and study design. Guang Liang and Xia Zhao participated in the drafting of the article. Lingyu She, Jinfeng Sun, Li Xiong, Ankang Li, Weili Li, Juan Ren, and Haibin Wu, carried out the experiments.

Author statement

All data were generated in-house, and no paper mill was used. All authors agree to be accountable for all aspects of work ensuring integrity and accuracy.

Supplementary material

Supplemental information includes 2 tables. All the other data are available from the authors on request.

Declaration of Competing Interest

The authors have no conflicts of interest to declare.

Acknowledgments

The study was supported by a grant from the Natural Science Foundation of Zhejiang province (LQ23H090018 to X.Z.), Zhejiang Provincial Key Scientific Project (2021C03041 to G.L.), and Hangzhou Medical College (00004F1RCYJ2109 to X.Z.).

Supplementary materials

Supplementary material associated with this article can be found, in the online version, at doi:10.1016/j.phymed.2023.155168.

References

Adlimoghaddam, A., Neuendorff, M., Roy, B., Albensi, B.C., 2018. A review of clinical treatment considerations of donepezil in severe Alzheimer's disease. CNS Neurosci. Ther. 24, 876–888. https://doi.org/10.1111/CNS.13035.

Bromley-Brits, K., Deng, Y., Song, W., 2011. Morris water maze test for learning and memory deficits in Alzheimer's disease model mice. J. Vis. Exp. https://doi.org/10.3791/2920.

Cai, Z., Yan, L.J., Li, K., Quazi, S.H., Zhao, B., 2012. Roles of AMP-activated protein kinase in Alzheimer's disease. Neuromol. Med. 14, 1–14. https://doi.org/10.1007/S12017-012-8173-2.

Daval, M., Ferré, P., Foufelle, F., 2006. AMPK, an active player in the control of metabolism. J. Soc. Biol. 200, 99–105. https://doi.org/10.1051/JBIO:2006013.

de Jesus de Paula, V.R., Meira Guimarães, F., Satler Diniz, B., Vicente Forlenza, O., 2009. Amyloid-beta, TAu protein or both? Dement. Neuropsychol. 3, 188–194.

Dong, W., Wang, F., Guo, W., Zheng, X., Chen, Y., Zhang, W., Shi, H., 2016. Aβ25-35 Suppresses mitochondrial biogenesis in primary hippocampal neurons. Cell. Mol. Neurobiol. 36, 83–91. https://doi.org/10.1007/S10571-015-0222-6.

Eftekharzadeh, B., Maghsoudi, N., Khodagholi, F., 2010. Stabilization of transcription factor Nrf2 by tBHQ prevents oxidative stress-induced amyloid beta formation in NT2N neurons. Biochimie 92, 245–253. https://doi.org/10.1016/J.BIOCHI.2009.12.001.

Elshafay, A., Tinh, N.X., Salman, S., Shaheen, Y.S., Othman, E.B., Elhady, M.T., Kansakar, A.R., Tran, L., Van, L., Hirayama, K., Huy, N.T., 2017. Ginsenoside Rk1 bioactivity: a systematic review. PeerJ 5. https://doi.org/10.7717/PEERJ.3993.

Fu, A.K.Y., Hung, K.W., Yuen, M.Y.F., Zhou, X., Mak, D.S.Y., Chan, I.C.W., Cheung, T.H., Zhang, B., Fu, W.Y., Liew, F.Y., Ip, N.Y., 2016. IL-33 ameliorates Alzheimer's disease-like pathology and cognitive decline. Proc. Natl. Acad. Sci. U. S. A. 113, E2705–E2713. https://doi.org/10.1073/PNAS.1604032113.

Giordano, G., Costa, L.G., 2011. Primary neurons in culture and neuronal cell lines for *in vitro* neurotoxicological studies. Methods Mol. Biol. 758, 13–27. https://doi.org/10.1007/978-1-61779-170-3_2.

Gouras, G.K., Almeida, C.G., Takahashi, R.H., 2005. Intraneuronal Abeta accumulation and origin of plaques in Alzheimer's disease. Neurobiol. Aging. 26, 1235–1244. https://doi.org/10.1016/J.NEUROBIOLAGING.2005.05.022.

Halliwell, B., 2006. Oxidative stress and neurodegeneration: where are we now? J. Neurochem. 97, 1634–1658. https://doi.org/10.1111/J.1471-4159.2006.03907.X.

Hardie, D.G., 2008. AMPK: a key regulator of energy balance in the single cell and the whole organism. Int. J. Obes. (Lond). 32 (Suppl 4), S7–S12. https://doi.org/10.1038/IJO.2008.116.

Hoover, B.R., Reed, M.N., Su, J., Penrod, R.D., Kotilinek, L.A., Grant, M.K., Pitstick, R., Carlson, G.A., Lanier, L.M., Yuan, L.L., Ashe, K.H., Liao, D., 2010. Tau mislocalization to dendritic spines mediates synaptic dysfunction independently of neurodegeneration. Neuron 68, 1067–1081. https://doi.org/10.1016/J.NEURON.2010.11.030.

Johnson, D.A., Johnson, J.A., 2015. Nrf2–a therapeutic target for the treatment of neurodegenerative diseases. Free Radic. Biol. Med. 88, 253–267. https://doi.org/10.1016/J.FREERADBIOMED.2015.07.147.

Joo, M.S., Kim, W.D., Lee, K.Y., Kim, J.H., Koo, J.H., Kim, S.G., 2016. AMPK facilitates nuclear accumulation of nrf2 by phosphorylating at serine 550. Mol. Cell. Biol. 36, 1931–1942. https://doi.org/10.1128/MCB.00118-16.

Kale, J., Osterlund, E.J., Andrews, D.W., 2018. BCL-2 family proteins: changing partners in the dance towards death. Cell. Death Differ. 25, 65–80. https://doi.org/10.1038/CDD.2017.186.

Kemp, B.E., Stapleton, D., Campbell, D.J., Chen, Z.P., Murthy, S., Walter, M., Gupta, A., Adams, J.J., Katsis, F., Van Denderen, B., Jennings, I.G., Iseli, T., Michell, B.J., Witters, L.A., 2003. AMP-activated protein kinase, super metabolic regulator. Biochem. Soc. Trans. 31, 162–168. https://doi.org/10.1042/BST0310162.

Kim, H.J., Jung, S.W., Kim, S.Y., Cho, I.H., Kim, H.C., Rhim, H., Kim, M., Nah, S.Y., 2018. Panax ginseng as an adjuvant treatment for Alzheimer's disease. J. Ginseng Res. 42, 401–411. https://doi.org/10.1016/J.JGR.2017.12.008.

Kornelius, E., Lin, C.L., Chang, H.H., Li, H.H., Huang, W.N., Yang, Y.S., Lu, Y.L., Peng, C. H., Huang, C.N., 2015. DPP-4 Inhibitor Linagliptin Attenuates Aβ-induced Cytotoxicity through Activation of AMPK in Neuronal Cells. CNS Neurosci. Ther. 21, 549–557. https://doi.org/10.1111/CNS.12404.

Kumar, P., Nagarajan, A., Uchil, P.D., 2018. Analysis of cell viability by the MTT assay. Cold Spring Harb. Protoc. 2018, 469–471. https://doi.org/10.1101/PDB.PROT095505.

Lee, S.M., 2014. Anti-inflammatory effects of ginsenosides Rg5, Rz1, and Rk1 : inhibition of TNF-α-induced NF-κB, COX-2, and iNOS transcriptional expression. Phytother. Res. 28, 1893–1896. https://doi.org/10.1002/PTR.5203.

Leirós, M., Alonso, E., Rateb, M.E., Houssen, W.E., Ebel, R., Jaspars, M., Alfonso, A., Botana, L.M., 2015. Gracilins: spongionella-derived promising compounds for Alzheimer disease. Neuropharmacology 93, 285–293. https://doi.org/10.1016/J.NEUROPHARM.2015.02.015.

Li, Z., Zhao, L., Chen, J., Liu, C., Li, S., Hua, M., Qu, D., Shao, Z., Sun, Y., 2020. Ginsenoside Rk1 alleviates LPS-induced depression-like behavior in mice by promoting BDNF and suppressing the neuroinflammatory response. Biochem. Biophys. Res. Commun. 530, 658–664. https://doi.org/10.1016/j.bbrc.2020.07.098.

Liu, D.Y., Li, Y.H., Xu, Y.T., Zhu, Y., 2016. Anti-aging traditional Chinese medicine: potential mechanisms involving AMPK pathway and calorie restriction based on "medicine-food homology" theory. Zhongguo Zhong Yao Za Zhi 41, 1144–1151. https://doi.org/10.4268/CJCMM20160629.

Lu, N., Tan, G., Tan, H., Zhang, X., Lv, Y., Song, X., You, D., Gao, Z., 2022. Maackiain prevents amyloid-beta-induced cellular injury via priming PKC-Nrf2 Pathway. Biomed. Res. Int. 2022 https://doi.org/10.1155/2022/4243210.

Markesbery, W.R., 1997. Oxidative stress hypothesis in Alzheimer's disease. free radic. Biol. Med. 23, 134–147. https://doi.org/10.1016/S0891-5849(96)00629-6.

Moneim, A., 2015. Oxidant/Antioxidant imbalance and the risk of Alzheimer's disease. Curr. Alzheimer Res. 12, 335–349. https://doi.org/10.2174/1567205012666150325182702.

Mota, S.I., Costa, R.O., Ferreira, I.L., Santana, I., Caldeira, G.L., Padovano, C., Fonseca, A. C., Baldeiras, I., Cunha, C., Letra, L., Oliveira, C.R., Pereira, C.M.F., Rego, A.C., 2015. Oxidative stress involving changes in Nrf2 and ER stress in early stages of Alzheimer's disease. Biochim. Biophys. Acta 1852, 1428–1441. https://doi.org/10.1016/J.BBADIS.2015.03.015.

Patel, S., Rauf, A., 2017. Adaptogenic herb ginseng (Panax) as medical food: status quo and future prospects. Biomed. Pharmacother. 85, 120–127. https://doi.org/10.1016/J.BIOPHA.2016.11.112.

Pei, H., Ma, L., Cao, Y., Wang, F., Li, Z., Liu, N., Liu, M., Wei, Y., Li, H., 2020. Traditional Chinese medicine for Alzheimer's disease and other cognitive impairment: a review. Am. J. Chin. Med. 48, 487–511. https://doi.org/10.1142/S0192415X20500251.

Pu, J.Y., Ramadhania, Z.M., Mathiyalagan, R., Huo, Y., Han, Y., Li, J.F., Ahn, J.C., Xu, F. J., Lee, D.W., Zeng, X.H., Yang, D.C., Kwak, G.Y., Kang, S.C., 2021. Ginsenosides conversion and anti-oxidant activities in puffed cultured roots of mountain ginseng. Process 9, 2271. https://doi.org/10.3390/PR9122271, 2021, Vol. 9, Page 2271.

Sandberg, M., Patil, J., D'Angelo, B., Weber, S.G., Mallard, C., 2014. NRF2-regulation in brain health and disease: implication of cerebral inflammation. Neuropharmacology 79, 298–306. https://doi.org/10.1016/J.NEUROPHARM.2013.11.004.

Shukitt-Hale, B., Bielinski, D.F., Lau, F.C., Willis, L.M., Carey, A.N., Joseph, J.A., 2015. The beneficial effects of berries on cognition, motor behaviour and neuronal function in ageing. Br. J. Nutr. 114, 1542–1549. https://doi.org/10.1017/S0007114515003451.

Slee, E.A., Adrain, C., Martin, S.J., 2001. Executioner caspase-3, -6, and -7 perform distinct, non-redundant roles during the demolition phase of apoptosis. J. Biol. Chem. 276, 7320–7326. https://doi.org/10.1074/JBC.M008363200.

Vorhees, C.V., Williams, M.T., 2006. Morris water maze: procedures for assessing spatial and related forms of learning and memory. Nat. Protoc. 1, 848–858. https://doi.org/10.1038/NPROT.2006.116.

Wu, J.jiao, Yang, Y., Wan, Y., Xia, J., Xu, J.F., Zhang, L., Liu, D., Chen, L., Tang, F., Ao, H., Peng, C., 2022. New insights into the role and mechanisms of ginsenoside Rg1 in the management of Alzheimer's disease. Biomed. Pharmacother. 152 https://doi.org/10.1016/J.BIOPHA.2022.113207.

Yeung, S.T., Martinez-Coria, H., Ager, R.R., Rodriguez-Ortiz, C.J., Baglietto-Vargas, D., LaFerla, F.M., 2015. Repeated cognitive stimulation alleviates memory impairments in an Alzheimer's disease mouse model. Brain Res. Bull. 117, 10–15. https://doi.org/10.1016/J.BRAINRESBULL.2015.07.001.

Zhang, Y., Yang, X., Wang, S., Song, S., 2019. Ginsenoside Rg3 prevents cognitive impairment by improving mitochondrial dysfunction in the rat model of Alzheimer's

disease. J. Agric. Food Chem. 67, 10048–10058. https://doi.org/10.1021/ACS.JAFC.9B03793.

Zhao, B., Lv, C., Lu, J., 2019. Natural occurring polysaccharides from Panax ginseng C. A. Meyer: a review of isolation, structures, and bioactivities. Int. J. Biol. Macromol. 133, 324–336. https://doi.org/10.1016/J.IJBIOMAC.2019.03.229.

Zheng, W., Chong, C.M., Wang, H., Zhou, X., Zhang, L., Wang, R., Meng, Q., Lazarovici, P., Fang, J., 2016. Artemisinin conferred ERK mediated neuroprotection to PC12 cells and cortical neurons exposed to sodium nitroprusside-induced oxidative insult. Free Radic. Biol. Med. 97, 158–167. https://doi.org/10.1016/J.FREERADBIOMED.2016.05.023.